

Article

Anguilliform Locomotion across a Natural Range of Swimming Speeds

Nils B. Tack, Kevin T. Du Clos and Brad J. Gemmell

Weighting the fish

The weight of the fish was measured in-vivo by temporarily (< 30 seconds) placing the fish in a dry re-sealable zipper bag. This prevented asphyxiation by maintaining the opercula closed (gills not directly exposed to air) and restrained the fish from moving, thus preventing injuries during the weighting process. The weight of the bag and the water that drained from the fish into the bag was subsequently subtracted from the total weight. After each pre- and post-experimental manipulation of the fish, a visual inspection was conducted to ensure that all the fins were intact.

Selection of videos

Videos were qualified for analysis if the fish were located no more than a body-width from the center of the test section in the y and z directions. This prevented potential wall effects caused by the proximity of the body of the fish to the walls of the test section. These constraints were not applicable to the x direction, but videos during which the fish was pushing on the upstream flow straightener and the downstream mesh were excluded from analysis.

Normalized body depth profile

In order to compute the pull and push components of thrust along segments of the body, a body-depth profile was established based on a picture of a fish swimming at a speed of 0.2 BL s^{-1} . The depth of the body was measured and normalized to body length at 12 points equally distributed along the length of the body (Figure S1).

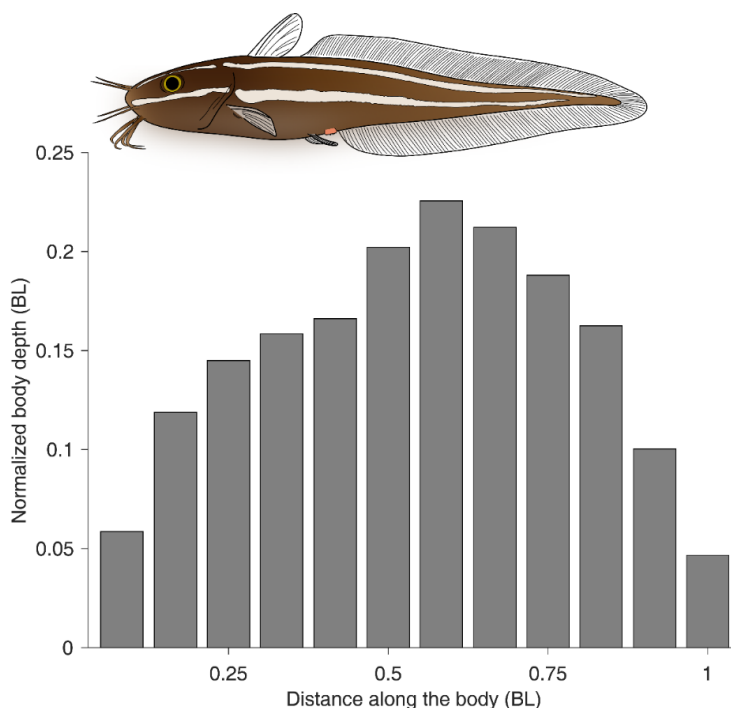


Figure S1. Normalized body depth profile of coral catfish.

Swim tunnel respirometer

Calibration

The calibration of water flow velocity to voltage output from the external motor driving the impeller generating the flow in the respirometer was performed using particle image velocimetry (PIV). Flow conditions in the test section of the swim tunnel respirometer were also assessed through PIV for speeds ranging from 0.06 m s^{-1} to 0.16 m s^{-1} . Velocity profiles were established for three equally distributed planes located at 1.7, 3.4, and 5.1 cm from the bottom of the test section (Figure S2). Vorticity fields revealed no identifiable flow artifacts in the test section. Only video sequences for which the fish were swimming between the lower and upper planes were selected for analysis. Additionally, the velocity profiles across the width of the test section revealed a uniform flow except along the edges of the walls for which the flow was slower (Figure S3). Only video-sequences for which the fish was near the center of the test section were selected for analysis.

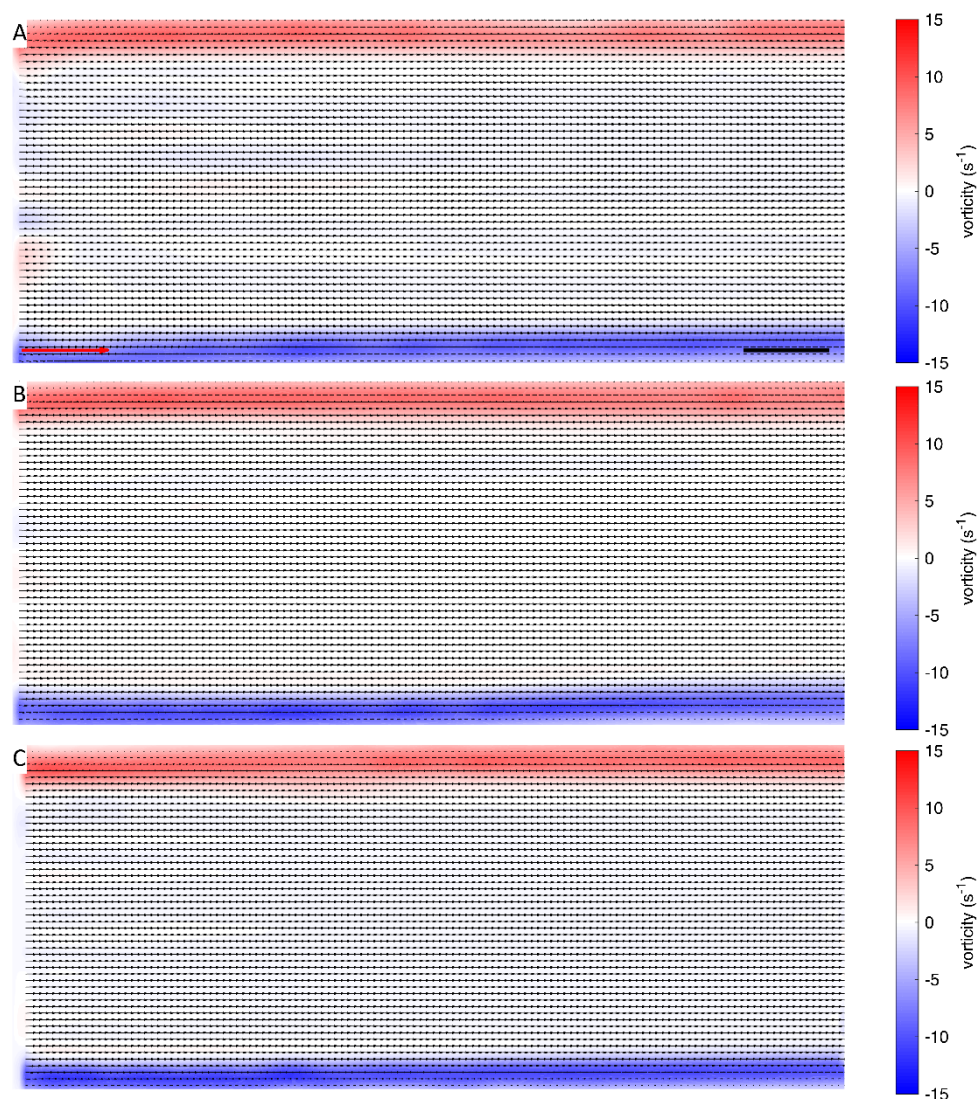


Figure S2. Velocity and vorticity fields of the cross section of the flume. No identifiable flow features were present in the test section across three equally distributed planes located at 1.7 cm (A), 3.4 cm (B), and 5.1 cm (C) from the bottom of the test section. Average flow speed $U=0.13 \text{ m s}^{-1}$. The red scale arrow indicates 1 m s^{-1} . The scale bars indicate 2 cm for all frames.

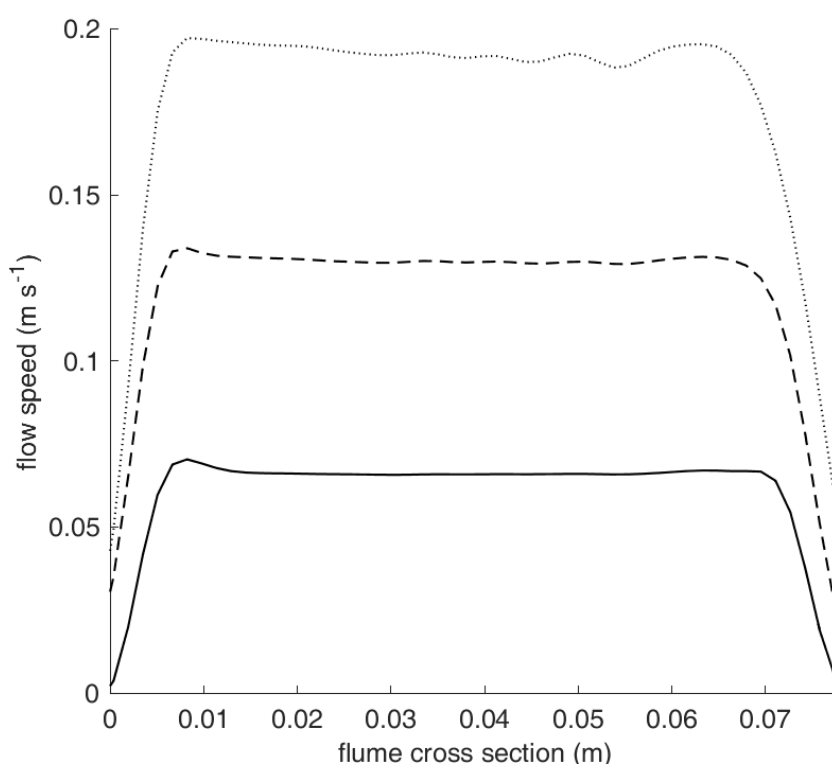


Figure S3. Velocity profile across the width of the test section for three speeds.

Respirometry

The swim tunnel respirometer was submerged in an aerated outer buffer tank maintained at ambient temperature ($21 \pm 1.0^\circ\text{C}$) that provided aerated water when flushing the swim tunnel respirometer during acclimation and after each closed measuring period. The respirometer was surrounded by blackout curtains to isolate the fish from external stimuli that could affect behavior and induce additional stress during the entirety of the experiments. Routine oxygen consumption rate was measured for 10 minutes under dim illumination conditions in a 0.395-liter flow through resting respirometer chamber submerged in an outer buffer tank maintained at ambient temperature ($21 \pm 1.0^\circ\text{C}$). This smaller respirometer prevented the fish from swimming actively against the flow, thus allowing for a more accurate measurement of routine oxygen consumption. These experimental conditions aimed at closely matching the natural flow and light conditions that juvenile coral catfish are subjected to when resting in crevasses or coral aggregates. During the respirometry experiments performed for swimming speeds ranging from 0.2 to 2.0 BL s^{-1} , an LED lamp (max output 2W) was placed above the downstream section of the swimming chamber to prevent the fish from resting against the downstream mesh. Additionally, this motivated the fish to occupy an upstream position as they exhibited negative phototaxis when placed in the swim tunnel. The flow-through respirometer loop used during respirometry experiments was fitted with a small pump (Sicce Syncra Nano, Pozzoleone, Italy) and a ball valve to deliver water to the optical oxygen sensor at a constant rate regardless of the swimming speed investigated. This eliminated any speed-dependent effects in the reading of the dissolved oxygen concentration by the oxygen probe.

Each fish transferred to the test section of the respirometer was allowed to recover from handling at a swimming speed $\leq 0.3 \text{ BL s}^{-1}$ and with fully aerated and thermoregulated seawater from the buffer tank for 4h prior to starting the experiment. The duration of this recovery phase was determined from the measurement of the resting metabolic rate over a period of six hours that reached an asymptote at about 4 hours after the transfer of the fish to the swim tunnel (Figure S4). Resting metabolic rate measure prior to starting any experiment showed no anomalies suggesting that temperature had a negative effect on the fish's performance and ability to acclimate.

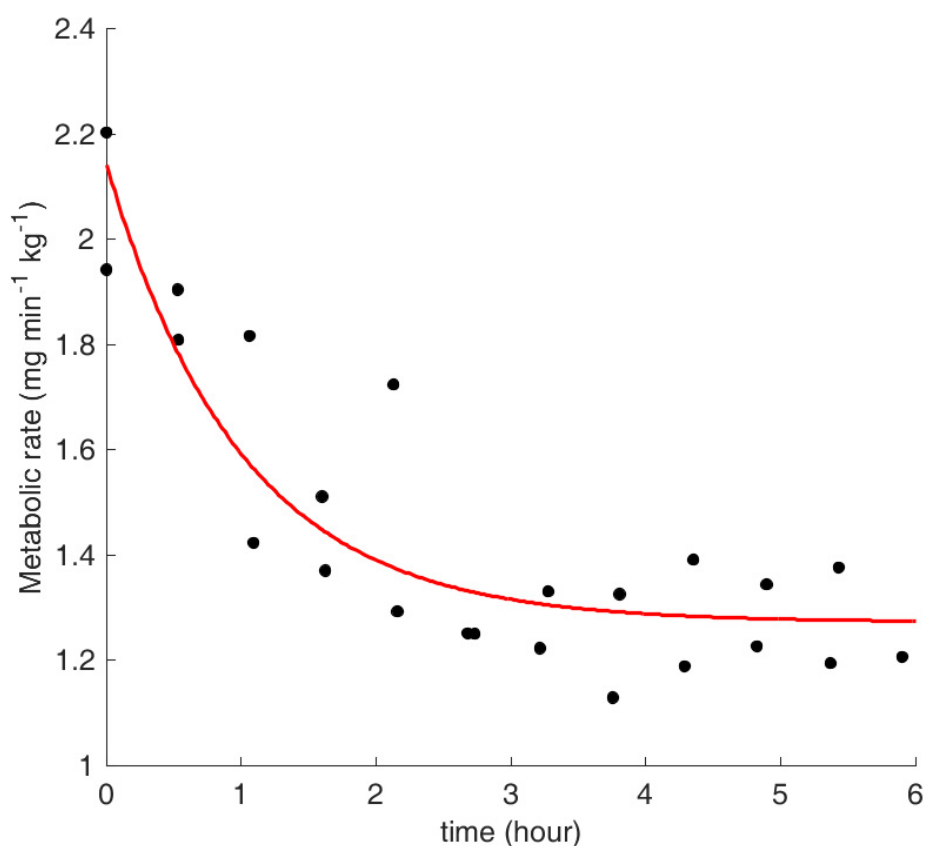


Figure S4. Recovery rate of the fish after handling. It is seen here through the stabilization of the measured resting metabolic rate ($\dot{M}O_{2,resting}$) over time. The equation for the fitted line (solid red line) is $\dot{M}O_{2,resting} = 0.8695 e^{-time} + 1.272$ ($R^2 = 0.8055$).

Horizontal divergence in the velocity vector fields

Because two-dimensional PIV data represent a projection of three-dimensional flow, it is important to characterize the impact of this limitation on the accuracy of the present results. The horizontal divergence in the velocity fields obtained from 2D PIV was calculated to provide additional evidence for the negligible effects of 3D flow features along the body and to further support the validity of the body-depth-corrected 2D PIV measurements of pressure fields and pull and push components of thrust. Horizontal divergence in the velocity fields (in the x - y plane) was calculated from the same velocity vector fields used to compute pressure fields according to the following equation using a custom program in MATLAB R2018a (MathWorks, Natick, MA, USA):

$$\nabla \cdot u = \frac{\partial u}{\partial x} + \frac{\partial v}{\partial y}$$

where u and v are the components of the vector field along the horizontal axes x and y , respectively. The velocity divergence was normalized with the velocity gradient, and the probability distributions of the normalized velocity divergence were calculated to show that no dominant 3D flow was present. Because the flows are incompressible, the fractional volume change is equal to zero when the flows are two-dimensional. Deviation from zero values can therefore be attributed to velocity gradients perpendicular to the plane of the velocity field. Divergence in the velocity fields is expected near the leading edge of the anal and dorsal fins during lateral body undulations. Although some divergence was observed along the rostro-caudal axis and above the rostro-caudal axis (along the dorsal fin), no major three-dimensional flow was identified, and the flow remains largely divergent-free (Figure S5). Divergence in the velocity fields can however be observed near the very end of the

caudal fin where the tail tapers abruptly (Figure S1). Because out-of-plane flows are negligible compared to the planar flow, and pressure effects dominate shear effects, the methods that we employed to compute experimentally derived pressure fields can reproduce the direction, magnitude, and timing of locomotor forces experienced by a fish relatively accurately [16].

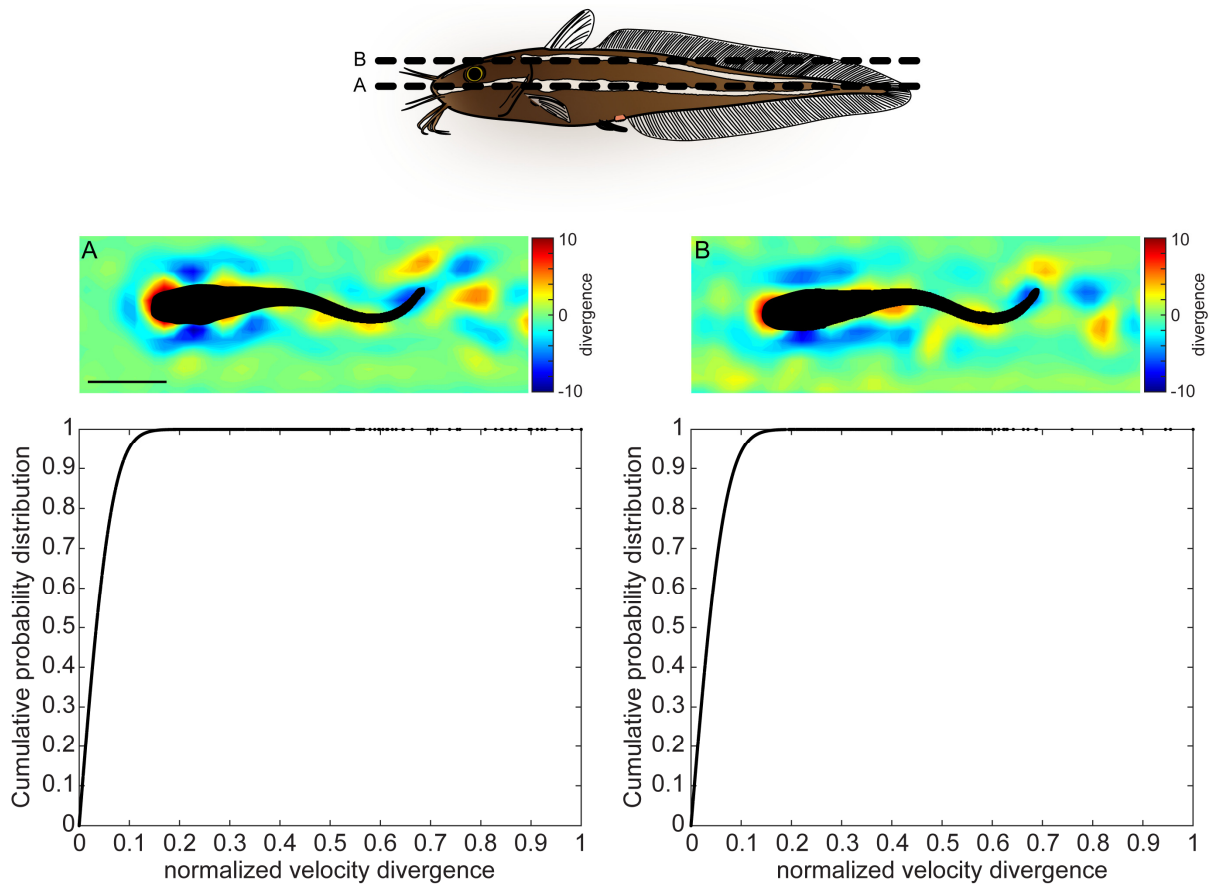


Figure S5. Divergence in the velocity vector fields and cumulative probability distribution of the normalized divergence. Divergence was computed along the rostro-caudal axis (A) and above the rostro-caudal axis, along the dorsal fin (B) at a swimming speed of 1.0 BL s^{-1} . Blue is sink (toward ventral side), red is source (toward dorsal side). The scale bars indicate 2 cm for both frames.